Exxon Valdez Oil Spill
Restoration Project Annual Report

Biophysical Modeling and Validation Through Remote Sensing

Restoration Project 97320-R
Annual Report

This annual report has been prepared for peer review as part of the *Exxon Valdez* Oil Spill Trustee Council restoration program for the purpose of assessing project progress. Peer review comments have not been addressed in this annual report.

David L. Eslinger

University of Alaska Fairbanks
Institute of Marine Science
Fairbanks, Alaska 99775

April 1998

SEA Trophodynamic Modeling and Validation Through Remote Sensing

Restoration Project 97320-R
Annual Report

Study History: This project is the result of an internal reorganization within the Sound Ecosystem Assessment (SEA) program. Some of the work performed under SEA core projects 95320-G and 95320-J in FY94 and FY95 has been done under this project since. We are continuing the trophodynamic modeling of phytoplankton and zooplankton begun in FY95, increasing the detail in the *Pseudocalanus* simulation, and adding modeling of ichthyoplankton, herring larvae in particular. We are evaluating and verifying the model against field data collected using a variety of remote sensing and *in situ* sampling platforms.

Abstract: Previous coupled physical and biological modeling of phytoplankton and zooplankton dynamics in Prince William Sound and the Gulf of Alaska have shown there to be two general types of response to different springtime physical dynamics. Warm, quiescent springs lead to brief intense phytoplankton blooms and relatively low zooplankton biomass, whereas, colder, stormy springs lead to longer phytoplankton blooms and higher zooplankton biomass. However, in FY97, further simulations with the model suggest that it is not simply the winds and temperature during the springtime, that determined what type of planktonic bloom would occur, rather, it is the interaction of springtime weather with the water mass left after the previous winter. A very warm winter produces results similar to a cold, windy spring: a slow phytoplankton bloom and a large zooplankton population. A very cold winter in turn, is similar to a warm spring, producing a brief, short phytoplankton bloom and low populations of zooplankton. These interactions occur because the phytoplankton bloom responds most strongly to the **stratification** of the water column, not to the temperature itself. The stratification process depends on the fluxes of heat, momentum, and salt into the upper water column. In early spring, the heat flux is largely determined by the temperature difference between the air and water. Therefore, a similar bloom occurs if the water is very warm, or the air is very cold. In FY-97, we completed and validated an N-by-one-dimensional model that accurately simulated these dynamics. This model is being expanded into the full three-dimensional domain during FY-98.

Key Words: biophysical modeling, biological oceanography, physical oceanography, phytoplankton, Prince William Sound, spring bloom, zooplankton

Citation: Eslinger, David L, Biophysical Modeling and Validation Through Remote Sensing, *Exxon Valdez* Oil Spill Annual Report (Restoration Project 97320-R), Alaska Department of fish and Game, Anchorage, Alaska.

Table of Contents:

Executive Summary 5

Introduction 6

Objectives 6

Methods 7

Results 8

Discussion 9

Conclusions 10

List of Tables, Figures, and Appendices:

Appendix A 11

Appendix B 19

Figure legends 25

Figure 1 26

Figure 2 27

Figure 3 28

Figure 4 29

Figure 5 30

Figure 6 31

Figure A-1 32

Figure A-2 33

Figure A-3 34

Figure B-1 35

Figure B-2 36

Figure B-3 37

Executive Summary:

As shown in the FY96 annual report, biophysical modeling of phytoplankton and zooplankton, in combination with field data collected as part of 320-G and 320-H, shows that phytoplankton and zooplankton populations in Prince William Sound and the northern Gulf of Alaska are determined by the winds and the differences between air and water temperatures which occur over a relatively short, critical time period in early spring. Although this critical time period may be as short as two weeks, the meteorological conditions occurring during that time will play a dominant role in the dynamics of the phytoplankton and zooplankton populations for the rest of the summer. Changes in the amount of convective mixing, caused by cold air, and of wind mixing, caused by high winds, during the early part of the phytoplankton bloom change the timing and duration of the bloom, the total primary production occurring during the bloom, and the partitioning of that primary production between the upper water column food chain, and the benthic food chain.

In FY97, we made significant expansions of the modeling work previously carried out. The model as described in the FY96 report is being expanded into a fully three-dimensional model. Several steps are necessary to produce a working, accurate 3-D model. We must have a reasonable model of Prince William Sound bathymetry; a set of realistic, spatially-varying wind fields; and a set of realistic currents with which to advect the plankton. The production of the realistic currents depends on the availability of the spatially varying winds. In FY97, we devised a method of using winds, measured at various stations within the PWS region, in conjunction with local knowledge of the effects of topographic steering, to develop a tool with which we can produce spatially varying wind fields. This method and tool are described below. We used the spatially-varying winds and the same model bathymetry as the physical modeling effort is using, to construct a three-dimensional model of plankton dynamics. We examined the effects of bathymetry and varying winds on the plankton populations. There were no results from the physical model available which used the spatially varying wind fields, therefore the plankton model does not include horizontal advection at the present time. The effects shown are due to local processes only. This type of model is commonly referred to as an N-by-one-dimensional model (Nx1D). We found that local effects are significant and that the Nx1D model does a reasonable job in simulating the results of field programs.

In addition to the Nx1D work, we made substantial improvements to the biological dynamics of the model through EVOS-supported graduate research by two students. Ms. Natalia Pintchouk is greatly expanding the *Pseudocalanus* zooplankton model. This work is described in Appendix A. Ms. Sarah Thornton is adding an ichthyoplankton (larval herring) component to the model. This work is described in Appendix B. Both of these students presented their work at the 1998 Ocean Sciences meeting in San Diego, CA, in February 1998. They attracted a good deal of attention for their work and received a great deal of praise. They will be finishing their projects and defending their theses in FY99.

Introduction:

Pacific herring and pink salmon have been identified as non-recovering resources injured by the *Exxon Valdez* oil spill. An ecosystem approach has been recognized by the EVOS Trustee Council as being necessary to reaching an understanding of the underlying processes and variables which may be constraining recovery of these injured resources. The currently proposed work is critical to the ecosystem study being undertaken by the SEA program. The role of the physical environment in controlling phytoplankton, zooplankton, and ichthyoplankton populations, and the role of these populations in the life history of Pacific herring and pink salmon, must be understood for the intelligent, informed planning of successful restoration efforts.

This project directly addresses the SEA pink salmon and Pacific herring restoration objectives. The phytoplankton and zooplankton serve directly as food for both herring and pink salmon at various life stages. Two large calanoid copepod species, *Neocalanus cristatus* and *N. plumchrus*, in particular, are thought to be potentially important as both a dietary item and a refuge from predation for pink salmon. Larval and juvenile herring feed on different stages of calanoid copepods, which reproduce throughout the spring and summer. The reproductive effort of these copepods is dependent on the timing, magnitude, and duration of the phytoplankton primary production in the spring bloom period and throughout the summer. The interactions between the various types of phytoplankton (*e.g.*, diatoms, flagellates) and zooplankton (*e.g.*, oceanic copepods, neritic copepods) varies both between and within years. The timing of the major increase in biomass of phytoplankton or zooplankton, sometimes called the spring phytoplankton or zooplankton bloom, respectively, may be important to the first feeding and subsequent survival of the larval herring and juvenile herring and salmon, *e.g.* Cushing's match-mismatch hypothesis. This project examines these issues through the use of numerical models, remote sensing, and field observations.

Results through FY-96 indicate that physical forcing dominates the dynamics at the lower trophic levels. The physical signal propagates up through the food chain and has relevant consequences months after the physical interaction actually occurred. These effects are highly nonlinear, but can be accurately simulated using the present model.

Objectives:

The major objectives to be achieved over the life of this project as detailed in the FY97 DPD were:

1. To construct a three-dimensional model of the physical/biological processes affecting phytoplankton, zooplankton, and ichthyoplankton dynamics in Prince William Sound.
2. To determine the relative roles of these processes in determining Pacific herring and pink salmon population levels.

3. To determine the spatial and temporal variability, both of the physical environment and of phytoplankton concentrations, using a combination of remote sensing techniques and field observations.

An additional minor objective was:

4. To deploy and maintain an upgraded version of the CLAB buoy, which will provide high temporal resolution time series of wind velocity, air temperature, surface water temperature, and subsurface temperatures at 10 depths. This will be the primary data source for the development of the physical/biological dynamics portion of the model.

These objectives will enable us to test the following hypotheses:

1. That coupling between the physical environment and phytoplankton dynamics can be modeled reliably.
2. That phytoplankton dynamics drive zooplankton dynamics in a predictable manner, which can also be modeled.
3. That the survival of larval herring can be estimated by a combination of modeling of larvae and field work on eggs and 0-class juveniles.
4. That interactions between the physical environment, the zooplankton field, and juvenile pink salmon populations can be predicted using a coupled biological/physical 3-D model.
5. That the spatial variability of the SST and chlorophyll concentrations in Prince William Sound, observed in satellite remote sensing images, can be simulated by a 3-D model of physical and biological dynamics.

Methods:

We are using a combination of coupled biological and physical models and satellite remote sensing data sets to achieve the above objectives. We are continuing the development of a coupled biological-physical model of lower trophic level, i.e. phytoplankton and zooplankton, dynamics for the near-surface layers of Prince William Sound (PWS). We have expanded the one-dimensional, depth-time model developed in FY-95 to include herring larvae. The 1-D model describes the biological and vertical processes that occur through time at a single location. The biological processes contained in the 1-D model are being integrated into a larger three-dimensional model with appropriate vertical resolution. The model is presently working in a Nx1D configuration, where only the local effects at each grid point are simulated. The Nx1D model contains bathymetry effects and spatially varying wind effects. This Nx1D model will become fully three dimensional when it incorporates the vector fields produced by the circulation model being constructed by V. Patrick and C. Mooers as part of 320-J. This will be done in FY98.

Spatially varying wind fields are needed to drive an accurate 3-D model. In conjunction with Vince Patrick, Jennifer Allen, and Stephen Bodner (all part of 97320J), we developed a methodology to use local knowledge from (initially) Cordovan pilots and fishermen to identify portions of the Sound which behaved similarly under different wind conditions. We could then take the measured winds over these areas and apply them to larger portions of the Sound. Again

in collaboration with Jennifer Allen (97320-J) we developed a JAVA-based tool to interactively do this. An example of the regions defined and the resultant wind field can be seen in Figures 1 and 2. Using this definition of the "wind regions" in the model, we ran simulations for 1995 and 1996.

The methodologies for the *Pseudocalanus* and ichthyoplankton models are given in Appendices A and B, respectively.

Our remote sensing work entails reception and processing of National Oceanic and Atmospheric Administration (NOAA) Nimbus series satellite data in Fairbanks, AK. Data from the NOAA Advanced Very High Resolution Radiometer (AVHRR) sensors are processed to produce sea surface temperature (SST) images of both the northern Gulf of Alaska and a more detailed image of Prince William Sound. In late 1997, the long-awaited OrbView-II satellite was launched, carrying the Sea-viewing Wide Field-of-view Sensor (SeaWiFS). Data from this satellite is received and processed at the University of Alaska Fairbanks. The data are available to NASA-authorized SeaWiFS users. We are authorized users and will be using the data to compare with model and field results in the future. Unfortunately, the Japanese ADEOS satellite, carrying another ocean color sensor, was lost due to power problems, and no data have become available to us covering Prince William Sound.

Results:

The results of the simulations using realistic bathymetry and spatially varying winds are shown in Figures 3 - 6. In Figure 3, average euphotic-zone phytoplankton concentrations can be seen to be varying due to local winds. Note the north-south gradient in concentration with highest values in the south, in the area we have been thinking of as the "River". This north-south gradient is similar to that observed by Peter McRoy's SEA phytoplankton project in 1995. Not too surprisingly, the model simulates a similar gradient occurring a bit later in zooplankton abundance (Figure 4), similar to that observed by Ted Cooney's SEA zooplankton project. In contrast, in 1996, phytoplankton are more uniformly distributed, with a smaller east-west gradient (Figure 5), again similar to that observed in the field data. Again, there is a similar gradient in the zooplankton model results. Both of these years were run with identical initial conditions and wind regions. The only differences were the air temperatures and wind velocities over the different regions. These model results show the importance of understanding the spatial gradients in winds, even over the relatively small scale of Prince William Sound.

Detailed results from the one-dimensional modeling work are given in the Results section of Appendices A and B. Briefly, from Appendix A, the *Pseudocalanus* model incorporates 15 different life stages into the model instead of the one stage previously used. This make a substantial difference in the amount of *Pseudocalanus* biomass that is available as food for larval herring. From Appendix B, we find that food availability plays a large role in the time it takes for larval herring to metamorphose to juveniles. This may have substantial effects on herring recruitment, as the larval stage is thought to be one of particularly high mortality. Therefore, it

appears that the inclusion of the *Pseudocalanus* life-stage details is an important factor if we hope to accurately predict herring recruitment.

We have been processing and archiving AVHRR SST since 1994, and presently have an archive of over 6,000 SST images available to the SEA project. These images are stored on 8 mm tape, CD-ROM, and hard disk. In early FY97, we delivered a subset of these images to the Prince William Sound Science Center (PWSSC) in CD-ROM format, for use by the PWSSC SEA investigators. In FY97, we processed and archived over 1500 SST images.

The measurable tasks which we proposed to perform in FY97 and the progress made are listed below.

- Begin ichthyoplankton model comparison with FY-96 field data. Model DONE, no larval herring field data collect by other groups.
- Recover C-LAB buoy. DONE
- Deploy C-LAB buoy for 1996 field season. DONE
- Collect, process, and analyze AVHRR images for 1997 field season. DONE
- Begin to collect, process and analyze ocean color from SeaWiFS and/or OCTS. Exact date of satellite launches TBD. INCOMPLETE: Satellites not operational in FY97. Presently underway.
- Complete FY-97 field collection efforts. DONE
- 3-D phytoplankton, zooplankton model complete, initial ichthyoplankton component working. 2/3 DONE: 3-D model awaiting vector forcing fields. Other components DONE.
- Complete analysis of AVHRR data from 1994-mid 1997. UNDERWAY, part of ongoing analysis.
- Annual report on FY-97 work. DONE

Discussion:

From the development of the Nx1D model, we can see the dramatic effect that local bathymetry and winds have on phytoplankton and zooplankton populations. Even in the simple simulations shown, with the wind regions constant, there were dramatic differences between the years due to local winds. The spatial patterns seen in the model results agree well with those seen in the field data from the phytoplankton and zooplankton components of SEA. These results underscore the importance of having accurate, spatially varying forcing fields if we are to understand and simulate the Prince William Sound Ecosystem.

Full discussions of the 1-D model results are presented in Appendices A and B.

Conclusions:

The three-dimensional, coupled bio-physical model being developed as part of this project is able to simulate the phytoplankton and zooplankton dynamics in the upper waters of Prince William Sound. In most years, this model requires measurements of only air temperatures and winds to accurately model the timing and magnitude of the phytoplankton and zooplankton blooms. The inclusion of additional life stages in the *Pseudocalanus* component seems justified, given the importance to larval herring survival of the timing and absolute amount of naupliar and younger *Pseudocalanus* copepodites available as food.

Appendix A

Modeling of Life Stage Dynamics of Pseudocalanus Spp. In Prince William Sound, Alaska.

Natalia M. Pintchouk and David L. Eslinger
Institute of Marine Science
University of Alaska Fairbanks

ABSTRACT

Springtime zooplankton populations in Prince William Sound, Alaska, are dominated by a number of species of calanoid copepods. These species can be loosely grouped into two categories: large *Neocalanus*-type copepods, which reproduce at depth; and smaller *Pseudocalanus*-type copepods, which reproduce at the surface, after feeding. The *Neocalanus*-type copepods are an important food source for pink salmon, pollock and other fish species in early spring. The *Pseudocalanus*-type copepods are an important food source throughout the spring, summer and fall, for larval and juvenile Pacific herring. Larval herring feed only on the smaller life stages of the *Pseudocalanus*-type copepods. The current study examines the effects of including life-stage information in simulating *Pseudocalanus* biomass.

We have developed a coupled biophysical model of plankton dynamics for Prince William Sound, Alaska. The model includes three potentially limiting nutrients: nitrate, ammonium, and silicon; two phytoplankton "species": diatoms and flagellates; and three zooplankton "species": the large *Neocalanus*-type of copepods, smaller *Pseudocalanus*-type copepod, and a euphausiid group. In the current study, we present a comparison of the results of the model using two different formulations for the *Pseudocalanus*-type of copepod. The first formulation combined all life stages in one variable, which simulated total *Pseudocalanus* biomass. For the second formulation, all stages of *Pseudocalanus* development were simulated. This required sixteen different variables, and resulted in a considerably more complicated model. Information on the biomass of different life stages is important in simulating the proportion of the total biomass available as food to Pacific herring.

BACKGROUND

Numerical modeling of phytoplankton, along with field data, shows that phytoplankton populations in Prince William Sound and the Northern Gulf of Alaska are determined by the winds and air temperatures which occur over a relatively short, critical time period in early spring. Changes in the amount of convective mixing, caused by the cold air, and of wind mixing, caused by high winds, change the timing and duration of the bloom. A relatively warm, quiescent

spring produces a relatively short and intense phytoplankton bloom. In colder years the bloom is prolonged due to mixing, which reduces phytoplankton concentrations and increases nutrient concentrations. Because zooplankton reproduce at much slower rates than phytoplankton, a prolonged phytoplankton bloom is beneficial to the zooplankton populations, resulting in higher zooplankton biomass. In other words, zooplankton biomass will be higher in colder years than in warmer years (Eslinger, 1997).

MODEL METHODOLOGY

I. *Pseudocalanus* Life cycle:

Development of *Pseudocalanus* includes next stages: embryo; naupliar stages NI-NVI; copepodites CI-CV and adults (CVI). As for taxonomic status, it was shown that different *Pseudocalanus* species had similar generation times (McLaren et al., 1989; Davis, 1983; Corkett and, McLaren, 1978).

1.1 Initial abundance:

The development of *Pseudocalanus* is assumed to be synchronous when the productive season starts with a population of animals that are largely at the same stage of development. In high latitudes synchrony of life cycles lead to synchronous spawning producing a number of cohorts of animals each with distinct characteristics. *Pseudocalanus spp.* in PWS has 1 yr life cycle.

The overwintered G0 generation is assumed to be comprised of CIV, CV copepodites, and adult females. Average abundance of animals in March for open sound stations for a number of years was reported to be 4.1, 11.7 and 22.2 animals per cubic meter respectively (Cooney, personal communication). However, these numbers vary substantially from year to year and from station to station. In the model, initial abundance for each present group was calculated from AFK data and was equal to 33:100:200 animals per cubic meter (CVI, CV, CVI respectively). These numbers were used for both model years 95 and 96, as initial total abundance from AFK hatchery data did not differ much for these years.

1.2 Reproduction: Number of eggs in clutches:

Overwintered adult fertilized females begin reproduce after they feed on spring phytoplankton, so that first clutch is laid around day 70. Minimum, mean and maximum number of eggs per clutch were set to be equal to 3 ,16, and 31 respectively (Corkett and McLaren, 1978).

1.3 Embryonic and stage development time; rate of production of sacks, and time between sucessesive clutches.

A female carries a sack until eggs are hatched and the time taken for embryos to develop is controlled by temperature and described by the Belehradec's function $EDT=a\cdot(T-\lambda)^b$, or $\log(EDT)=\log(a) + b\cdot\log(T-\lambda)$,where EDT is embryonic development time in days, T is water temperature in C; b=-2.05 is the slope of the line, b is constant and assigned arbitrary; a is an intercept on the y-axis is shown to be related closely to egg size (Corkett and McLaren, 1978); λ

varies with temperature and is called the biological zero since on linear plot it is theoretical temperature at which EDT is infinite.

Parameters of Belehradec's function were calculated for few locations (Corkett and McLaren, 1978). Coyle, Paul and Ziemann (1990) reported that for south central Alaska (Auke bay), the equation for embryonic development was similar to that for the North Sea EDT=1845*(T+11.45)-2.05 and that the above equation predicted a generation time of 64 days at 5C which was similar to their estimate from cohort data. This equation was used in the model. Temperature data (2hrs interpolation) was calculated from Pollard-Thompson mixed layer model

It was estimated that fertilized females can reproduce up to 8-10 times. Corkett , McLaren (1978) summarized results obtained by Thompson (1976; cited by Corkett and, McLaren, 1978) and Paffenhofer, Harris (1976) and assumed that the successive clutches appear at intervals equal to about 1.25 times the duration of embryonic development for the given temperatures. New clutch is laid only if there is enough food for female to get excessive biomass equal at least to the difference between female base weight and minimum egg sack weight.

There is no agreement whether developmental time per stage is a function of temperature only, or if it also depends on food concentration, or if there is a compound effect of these two factors and how big the effect may be. Corkett and McLaren (1978), Huntley, Lopez (1992) assumed that stage development time was a function of temperature only, that micro-patches of food in the sea enabled copepods to graze efficiently and to grow at max rates. Ohman (1985) for Dabob Bay, Washington, and Evans (1981) for the North Sea also reported that food did not seem to influence body size, growth, development and reproduction of *Pseudocalanus*. In case of excess amounts of food, development times for different stages is only a function of temperature and may be approximated from embryonic development time.

Corkett and McLaren (1978) for the populations from Nova Scotia, and Thompson (1976; cited by Corkett and McLaren, 1978) for the populations from the North Sea found that development is roughly isochronal for all copepodids stages and that all copepodide stage has about the same duration as embryonic duration at any temperature. However, stage development time is not isochronal for naupliar stages, and for the North Sea it was estimated that duration of NI, NII, NIII, NIV, NV, and NVI stages was respectively .18, .37, 1.46, .81, .69 and .4 times EDT (Corkett and McLaren, 1978).

In our model, females reproduced 8 times when food was available; females were considered to be reproductive throughout of their life time span. For every cohort entering the pool of reproductive females (sex ratio of molting CV's was set to be 1:1), its ratio to a total number of reproductive females was calculated. Keeping mortality rates stage-specific but constant throughout the reproductive season, it was possible to keep track of the cohort structure of reproductive females and back calculate the proportion of females replenishing the pool of old nonreproductive females. Model shortest time interval between successive clutches was set equal to 1.5*EDT which corresponded to the longest stage duration time. This avoided temporal

overlap between successive broods. The duration of development stages was set as it was reported by Corkett and McLaren (1978).

2. *Pseudocalanus spp.* metabolism:

2.1 Weight estimates

Wet weights (mg) are available only for copepodid and adult stages (Cooney, Coyle, personal communication). Naupliar weights were taken from Hay, Evans (1988), and multiplied by 2.5 because PWS *Pseudocalanus* are, in average, 2.5 times bigger then those of the North Sea.

TABLE 1: *Pseudocalanus* weight, ug dry wt

size	Hay,Evans(1988),10C	Vidal(1988), 10C	Cooney and Coyle (1996)
Egg	.304		.760 (2.5*.304 from Hay)
NI	.304		.760 (2.5*.304 from Hay)
NII	.367		.918 (2.5*.367 from Hay)
NIII	.498		1.246 (2.5*.498 from Hay)
NIV	.616		1.540 (2.5*.616 from Hay)
NV	.730		1.826 (2.5*.730 from Hay)
NVI	.809		2.022 (2.5*.809 from Hay)
CI	.551		1.650
CII	1.134	1.5	2.850
CIII	2.128	3.0	5.294
CIV	3.712	5.0	7.950
CV	5.968	7.0	13.126
AF	10.349	10.0	31.350
AM	5.339		9.900

In the model weight for each developmental stage is recalculated at every time step from

biomass estimates and abundance.

2.2 *Pseudocalanus* stage-specific growth rates

A simple growth model was developed to estimate net increase in *Pseudocalanus* biomass. Maximum growth rate for each feeding stage was determined as a difference in maximum weights between the successive stages times reciprocal of stage duration time, and was approximated by the exponential function of temperature. Growth rate for feeding adult female

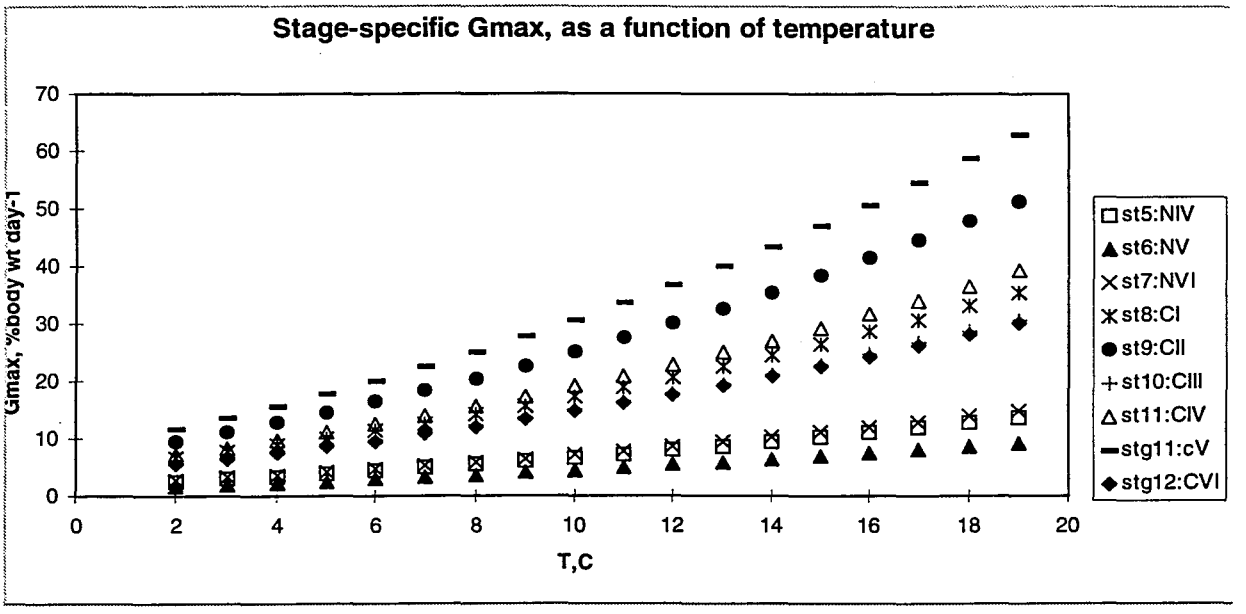

was defined in a similar way, but upper weight limit was defined as the maximum weight a female can achieve if she carried an egg sack of maximum size(31 eggs). Time to achieve this weight when food is abundant should then be equal to the time between successive clutches, i.e.1.5*EDT. Nonreproductive old females and males just maintained balance (growth=ingestion-respiration-egestion) near zero levels, i.e. they did not grow. Food limitation did take place in the system after day 180 (the end of June), and was accounted for in mortality stage-specific pressure.

2.3 Pseudocalanus metabolic costs

Nitrogen losses are in the form of ammonia and are modeled by a weight-specific empirical equation developed for boreal zooplankton species by Dagg et al. (1982): $U=.072W^{.902}$, µgN/cop/day. In the model, the ammonia term was added to a nutrient pool.

2.4 Egestion

Conover (1968; cited by Magley, 1990) first found that herbivorous zooplankton assimilated phytoplankton with 60 to 95% efficiency. In the model, assimilation efficiency was set equal to

75% . The egestion term was added to the detritus pool.

2.5 Molting, % of content of body weight:
Vidal (1980) estimated for *C. pacificus* that molting costs were between 2 and .2% of carbon content of body weight. In the model, it was set to 0.5 of *Pseudocalanus* body weight

2.6 Mortality
Most of the available methods for estimating mortality rates for stage-structured zooplankton populations assume that mortality rates are either constant throughout time, uniform across stages, or both. But different stages respond in different ways to changes of temperature, food availability, and their predators remove size selected classes. Ohman and Wood (1996) used a population surface method to get average stage-specific total mortality estimates throughout the reproductive season. In the model, stage-specific mortality estimates followed the general pattern obtained by Ohman and Wood (1996) but varied in magnitude. The potential larval herring feeding pressure was excluded from mortality estimates before larvae herring entered the system (julian day 135).

TABLE 2: Instantaneous stage-specific mortality (d-1) for *Pseudocalanus*, averaged through the reproductive season (from Ohman, Wood, 1996)

Eggs	NI-NVI	CI	CII	CIII	CIV	CV	AF	AM
.0525	.11	.15	.07	.045	.06	.1	.0525	.55

RESULTS AND DISCUSSION

We have developed 1-D coupled biophysical model of plankton dynamics which simulates all life stages of *Pseudocalanus spp.* The model is tuned for 1995 and 1996, the first being a year when copepod biomass was high (including *Pseudocalanus spp.*), and the second, a low year. Good agreement is achieved between two model formulations, without and with *Pseudocalanus* life stages (Figure A-1). Results from modeling stage-specific *Pseudocalanus spp.* dynamics provide information on food availability for Pacific herring over the spring bloom (Figure A-2). It was reported that the earliest life-stages of marine fish have a substantial impact on the population dynamics of *Pseudocalanus spp.* (Bollens S.M., 1988; Hay S.J. et all., 1978). At present, our model stage-specific mortality estimates are similar to those obtained by Ohman and Wood (1996) for *Pseudocalanus* populations from the Dabob Bay, WA. To fit modeled *Pseudocalanus* biomass to the field data, first, potential larvae herring pressure was removed from the system before the day 135, when larvae herring enter the system; and second, stage-specific mortality in 1996 was set to twice that for 1995, causing about a threefold decrease in *Pseudocalanus* biomass (Figure A-1, A-3). At present, the simple growth model is structured to estimate the total *Pseudocalanus* increase in biomass; *Pseudocalanus* grows at maximum rates.

However, food limitation may occur in the system after spring phytoplankton bloom is exhausted (Eslinger, 1997) and we assume that it will be one of the components of stage-specific mortality pressure along with invertebrate and vertebrate predation. Figure A-3 shows that the difference in total *Pseudocalanus* biomass in years 1995 and 1996 is mainly due to the difference in adult female biomass. Food limitation is the likely factor controlling adult female abundance. In year 1995 there is distinct secondary *Pseudocalanus* bloom followed by high summer abundance of adult reproductive females. Food limitation and stage-specific mortality pressure from Prince William Sound field data are not included in the formulations.

REFERENCES

Bollens S.M. 1988. A model of the predatory impact of larval marine fish on the population dynamics of their zooplankton prey. In: J. Plankton res., v.10, n.5, pp. 887-906

Cooney R.T., and K.O. Coyle. 1996. The role of zooplankton in Prince William Sound Ecosystem. In: SEA - An Integrated Science Plan for the Restoration of Injured Species in Prince William Sound, FY 1995 Annual Report; Chapter 5.

Corkett C.J, and McLaren I.A. 1978. The biology of *Pseudocalanus.* In: Russel, F.A. and Yonge, M (eds) Advances in Marine Biology. Academic Press, New-York, V.15, pp.1-231

Coyle K.O., A.J. Paul, and D.A. Ziemann. 1990. Copepod populations during the spring bloom in an Alaskan subarctic embayment. In: J. of plankton Res., V.12, N.4, pp.759-797.

Dagg M. J., J. Vidal, T.E. Whitledge, R.L. Iverson and J. J. Goering. The feeding, respiration, and excretion of zooplankton in the Bering Sea during a spring bloom. In: Deep-Sea Res., v.29, n.1a, pp.45-63, 1982.

Davis C.S. 1983. Laboratory rearing of marine calanoid copepods. J. Exp. Mar. Biol. Ecol., 71,pp.119-133

Eslinger D.L. 1997. Biophysical modeling and validation through remote sensing. In: Exxon Valdez Oil Spill Annual Report (Restoration Project 96320-R), Alaska Department of Fish and Game, Anchorage, Alaska.

Evans, F. 1981. An investigation into the relationship of sea temperature and food supply to the size of the planktonic copepod *Temora longicornis* Muller in the North Sea. In: Estuar. coast. Shelf Sci. 13: 145-158.
Hay S.J.,Evans G.T, Gamble J.C. 1988. Birth, growth and death rates for enclosed populations of calanoid copepods. In: J. Plankton Res., v.10, pp. 431-454.

Huntley M.E., Lopez M.D.G. 1992. Temperature-dependant production of marine copepods: a

global synthesis. In: Am. Nat., v.140, pp.201-242.

Magley C.W. 1990. A phytoplankton-zooplankton model of the middle and outer shelf domains of the southeast Bering Sea shelf during spring bloom conditions. PhD thesis. The Florida State University. College of Arts and Sciences.

McLaren I.A., Sevigny, J.M., and Corkett, C.J. 1989. Temperature-dependant development in *Pseudocalanus* species. In: Can. J. Zool., v.67, pp.559-564.

Ohman M.D. 1985. Resource-satiated population growth of the copepod *Pseudocalanus sp.* In: Ergeb. Limnol., v.21, pp. 15-32.

Ohman M.D, Wood S.N. 1996. Mortality estimation for planktonic copepods: *Pseudocalanus newmany* in a temperate fjord. In: Limnology and Oceoanography, v.41, n.1, pp.126-135.

Paffenhofer, Harris. 1976. Feeding, Growth and Reproduction of the Marine Planktonic Copepod *Pseudocalanus elongatus* Boeck. In: J. Mar.biol. Ass. UK, V.56, pp. 327-344.

Pollard R.T., C.L. Gallegos, and W.G. Harrison. 1973. The deepening of the wind-mixed layer. In: Geophysical Fluid Dynamics, n.4, pp.381-404.

Vidal.1980. Physioecology of zooplankton. 1. Effects of phytoplankton concentration, temperature, and body size on the growth rates of *Calanus pacificus and Pseudocalanus spp.* In: J. of Marine Biol., n.56, pp. 111-134

Vidal J. 1980. Physioecology of zooplankton. 2. Effects of phytoplankton concentration, temperature, and body size on the development and molting rate of *Calanus pacificus and Pseudocalanus spp.* In: J. of Marine Biol., n.56, pp. 135-146

Appendix B

Effects of Environmental Variability on the Growth of Larval Pacific Herring in Prince William Sound, Alaska

Sarah J Thornton and David L Eslinger
Institute of Marine Science
University of Alaska Fairbanks

Justification

As part of SEA, we have developed a biophysical model of Prince William Sound which accurately simulates lower trophic level dynamics. Here, we present the results of continued modeling work examining the early life history of Pacific herring. Herring dynamics are modeled in conjunction with the biophysical model of phytoplankton and zooplankton dynamics.

Abstract

Growth and survival of larval Pacific herring, *Clupea pallasi,* are simulated for 1993 through 1996 using a larval dynamics model coupled to a biophysical model of plankton dynamics in Prince William Sound, Alaska. The biophysical model, a one-dimensional (z,t), high-resolution plankton model forced by measured meteorological data, closely reproduces the spring phytoplankton bloom and subsequent zooplankton population development in Prince William Sound. The herring model is forced by physical and zooplankton results from the biophysical model and is used to examine the influence of oceanographic processes on the growth and survival of Pacific herring larvae. Small changes in mixed layer temperature and zooplankton concentrations during the larval period lead to substantial differences in the larval stage duration. Larval herring are modeled from hatching through metamorphosis to the juvenile stage. The herring model includes feeding, growth, metabolic costs, starvation and predation components. The model is initialized with hatch date estimates and results are compared with juvenile herring characteristics. We have examined the response of Prince William Sound larval herring to environmental variability and different forcing scenarios. The implications of our results to understanding Pacific herring recruitment variability is discussed.

Introduction and Background

Coupled physical and biological modeling of phytoplankton and zooplankton dynamics in Prince William Sound have shown there to be two general scenarios of springtime dynamics. Warm, quiescent springs lead to brief, intense phytoplankton blooms, whereas colder, stormier springs lead to longer phytoplankton blooms. These two types of phytoplankton blooms produce substantially different zooplankton blooms. The brief, intense blooms occur too quickly for much biomass to be transferred into the upper trophic levels. Therefore, the following zooplankton

bloom is substantially lower. In contrast, the longer duration phytoplankton bloom allows time for the zooplankton to "catch-up" and produce high zooplankton concentrations.

Larval herring feed on certain stages of small calanoid copepods, which reproduce throughout the spring and summer. The reproductive effort of these copepods is dependent on the timing, magnitude, and duration of the phytoplankton primary production in the spring bloom period and throughout the summer. The interactions between the various types of phytoplankton (*e.g.*, diatoms, flagellates) and zooplankton (*e.g.*, oceanic copepods, neritic copepods) varies both between and within years. The timing of the major increase in biomass of phytoplankton or zooplankton, sometimes called the spring phytoplankton or zooplankton bloom, respectively, may be important to the first feeding and subsequent survival of the larval herring. Results through FY96 indicate that physical forcing dominates the dynamics at the lower trophic levels. The physical signal propagates up through the food chain and has relevant consequences months after the physical interaction actually occurred. We have constructed these simple models of larval herring dynamics to examine the possible implications of these lower trophic level differences on herring growth. Are the interannual differences manifested in the growth rates and larval period duration of the herring?

Model Methodology

Herring are modeled from hatch in the planktonic stage through metamorphosis to the juvenile stage. Herring in the Bering Sea, Southeast Alaska, and British Columbia metamorphose at 25 to 30mm in length, regardless of age. Prince William Sound herring hatch in mid-May as yolk-sac larvae and by mid-July are found as juveniles in juvenile nursery areas. As a target for the model, we use a length of 25mm for metamorphosis, and calculate the time for the average fish to reach 25mm. We use 60 days as a reference point at which to judge size-at-age. Larvae hatch as yolk-sac larvae and begin to feed after 48 degree-days have passed.

The models are forced by the biophysical model results of mixed layer temperature and small calanoid copepod biomass. Herring larvae are known to eat smaller calanoid copepods, for example *Pseudocalanus* spp. The biophysical model does not simulate age-structure in the small calanoid (Pseudocalanus-type) population. As herring larvae can only eat the smaller stages (eggs and naupliar stages, copepodites for the late larvae) a fraction of the Pseudocalanus-type biomass is considered to be available for the larvae to consume. This fraction is set such that in an intermediate year (1995) larvae reach 25mm in 60 days, in agreement with field data. For the purpose of this discussion, 55% of the Pseudocalanus biomass is considered to be small enough for the larvae to eat. Annual copepod levels fall into two categories: 1993 and 1996 are low years, 1994 and 1995 are high years. Over the larval period, from hatch in May through the summer, zooplankton biomass shows a gradual decline from peak levels (Figure B1). Mixed layer temperature is relatively similar in all modeled years (1993-1996). Temperatures in the mixed layer range from 5 to 15°C with a gradual warming over the larval period. The warmest year was 1993.

The models include feeding, metabolic costs, and mortality due to predation. Food consumption

is approximately 25% of the fish biomass per day, up to the maximum field-observed zooplankton mortality. Feeding and metabolic rates are a function of temperature. Predation mortality is set at 4% of the fish biomass daily. Feeding occurs only during the day on a 16:10 light:dark cycle.

Depth-integrated model:
The depth-integrated model is a stand-alone, point model which is forced by outputs from the biophysical model. The model simulates larval growth for 1993, 1994, 1995 and 1996. Food concentrations are the average biomass of small calanoid zooplankton if evenly distributed over the top 40m of the water column. Sensitivity analyses are conducted on the depth-integrated model to examine temperature and food effects on growth rates. Sensitivity trial 1 involved modifying the amount of food available to the larvae by ±20%. The biophysical model does not include *Pseudocalanus*-type age-structure. The relative proportion of the smaller stages of Pseudocalanus-type copepods is unknown at this time, although another modeling effort is working on this problem. The model was run at both higher and lower food availabilities. Sensitivity trial 2 involved modifying the mixed layer temperature by ±2 °C.

Depth-resolving model:
The depth-resolving model examines the different growth conditions felt by larvae at discrete depths in the water column. It is an enhancement of the biophysical model, and as such, feedback occurs as the larvae consume some of the zooplankton biomass. Larvae are distributed in the upper 50m of the water column, with the same number in each depth-interval. Larvae do not vertically migrate and are not mixed by physical processes, but maintain their position in the water column. Zooplankton are mixed. The model is run for 1995 and 1996 using the same meteorological forcing conditions as the depth-integrated model.

Results

Depth-integrated model results
Using depth-averaged small-sized calanoid biomass, herring growth in all years is similar until the larvae are 40 days old (day 165) (Figure B2). In 1993 and 1996, growth slows due to food limitation after day 165. Table I gives a summary of the growth rate, size-at-age, and larval period duration for each of the test years. Growth rates (% of mass gained per day) vary by a factor of two between the 'high' and 'low' food years and fall within the range of literature values for field and laboratory-reared Pacific and Atlantic herring larvae. The time for the larvae to reach 25 mm ranges from 50 to >100 days. The two food scenarios produce two results. Years with higher food have larger larvae which reach metamorphosis earlier. Years with lower food concentrations have slower growing larvae which reach metamorphosis later. 1995 larvae reach metamorphosis (25mm) almost a month earlier than the 1996 larvae.

Table I: Summary table for 1993 through 1996 specific growth rates ($\%d^{-1}$), size at 60 days (mm) and the time to reach metamorphosis (d).

	1993	1994	1995	1996
Growth rate ($\%d^{-1}$)	3.3%	6.1%	5.7%	4.5%
Length-at-age60 (mm)	18.2	26.4	25.1	21.4
Larval stage duration (d)	>100	55	60	88

Sensitivity analyses for depth-averaged model

Food availability:

Differences were seen in all measured parameters, including the larval period length and larval growth rates (Table II). Higher food availability increases growth rates and length at 60 days for all four years. In the years in which food was more limiting (1993 and 1996) an increase in food shortened the larval period by up to 6 days. However, in years with higher food abundance (1994 and 1995), the difference in larval stage duration was very small under both higher and lower food availability.

Table II: Summary table for sensitivity trial 1, food availability, showing the larval stage duration (d) under three food levels.

	1993	1994	1995	1996
- 20%	>100	58	64	94
no offset	***>100***	***55***	***60***	***88***
+ 20%	96	55	58	82

Temperature:

In the second experiment, the model was run at mixed layer temperatures of 2°C higher and lower than actual. Temperature has many effects on Prince William Sound dynamics, affecting food concentrations available to larval fish. In this model, temperature also affects larval herring feeding rates and metabolic rates, following a Q_{10} relationship. Higher temperatures increase metabolic costs and maximum feeding rates for the larvae. In the poor food years (1993, 1996), the larvae are food-limited and therefore cannot increase the feeding rate. Metabolic rates increase under the higher temperatures, resulting in depressed growth rates and size-at-age. The larval stage duration increases by a few days (Table III). In the higher food years (1994, 1995), there is little or no food limitation, so both feeding and metabolic rates increase. Growth rates and the larval size-at-age are slightly higher due to more feeding. Cooler temperatures decrease the metabolic costs felt by the larvae, but also decrease the maximum feeding rate. In years of

poor food concentrations, the growth rates are slightly enhanced by the cooler temperatures. In years of higher food concentrations, there is a dramatic increase in the larval stage duration (8-10 days) due to a reduction of the non food-limited growth rates by ~1%/d.

Table III: Summary table for sensitivity trial 2, mixed layer temperature, showing the larval stage duration (d) under three temperature regimes.

	1993	1994	1995	1996
- 2°C	99	65	68	85
no offset	***>100***	***55***	***60***	***88***
+ 2°C	>100	51	56	91

Depth-resolving model results

In the depth-resolving model, small calanoid copepods are concentrated at the depth of the chlorophyll maximum. Larval growth is greatest in the areas of concentrated zooplankton (Figure B3). In 1995, a deep mixed layer results in significant zooplankton biomass down to 40m. Larvae in the top 40m are able to feed and grow. Larval growth continues in the surface 25m after 60 days. In 1996, a shallower mixed layer keeps the zooplankton biomass in the surface 25m. No larval growth occurs below 25m. After 60 days, food becomes limiting at all depths except 15-25m. The position of larvae in the water column has a large effect on the growth rate, size-at-age, and larval stage duration. Herring food is not evenly distributed in the water column; there is vertical structure to the zooplankton community. A further enhancement of the model will be to add herring vertical migration.

Discussion

Subtle changes in spring weather determine summer plankton dynamics in Prince William Sound. Interannual differences exist in the timing, magnitude, and duration of the spring phytoplankton and zooplankton blooms. We have constructed these simple models of larval herring dynamics to examine the possible implications of these lower trophic level differences on herring growth. Are the interannual differences manifested in the growth rates and larval period duration of the herring?

We have constructed simple models of larval herring dynamics representing the fate of the average fish each year. All modeled larvae eat the same proportion of the calanoid population. When herring larvae are small, only the smaller life-stages of the calanoids are small enough for the fish to eat. As the larvae grow, their gape widens and larger stages become available for consumption. The size-structure of the calanoids will also change over the season as reproduction occurs. The current biophysical model does not include this size- or stage-structure for the small calanoid population (see Pintchouck and Eslinger for a version which includes the age-structure). We have scaled the model such that in an intermediate year (1995), the larvae are able to reach metamorphosis in 60 days. As a result, 55% of the calanoids are assumed to be an appropriate

size for the larval herring to eat.

Initial growth rates are similar in 1993 through 1996. All fish are growing at maximum rates, with interannual differences in growth rate controlled by temperature. The zooplankton concentrations are high in the initial days of the larval period. Food limitation occurs later in the larval period, not at first-feeding. As the fish grow, they require more food. In the years with lower food concentrations, the larvae become food limited and their growth slows. In 1993, limitation begins by the time the larvae are 20 days old. In 1996, the higher zooplankton concentrations allow unlimited growth until the larvae are about 30 days old. The larvae continue to feed under these lower food concentrations, but they cannot eat as much, and therefore grow slower. These fish take much longer to reach metamorphosis size. If these growth conditions mimic the true case in Prince William Sound, it can be seen that in years with lower zooplankton concentrations, herring will spend longer in the vulnerable larval stage.

The sensitivity analyses help to clarify the relative effects of temperature and food on larval growth. As expected, when the concentration of food is increased in low-food years, the limitation is eased and growth rates increase. In the high-food years (1994, 1995), decreasing the available biomass of food by 20% does decrease the growth rates. A change of only 20% causes a 3-4 day increase in the larval period, showing that the larvae in 1994 and 1995 were close to food limitation in the base case. When food is not a limiting factor, increasing the temperature can decrease the larval period duration by enhancing growth rates over the increased metabolic costs. If fish are food-limited, however, increasing the temperature can cause drastic decreases in a growth rate due to higher metabolic costs. In 1993, larvae were both food-limited and experiencing the warmest temperatures of the four model years. The 1993 larvae had the lowest growth rates and took over four months to reach 25mm in length. Metamorphosis did not occur in the model until late September.

After metamorphosis to the juvenile stage, the herring are much more motile, actively swimming in pursuit of prey and in avoidance of predators. A larger size range of food particles is available to the fish. The juveniles have only a short time to store energy for the coming winter, when zooplankton have very low standing stocks. There is limited food available to the juvenile herring. The better their condition entering the overwintering period, the greater their chance of surviving the near-fast conditions they experience until the following spring zooplankton bloom. Therefore, the longer the larval period, the harder it is for the juveniles to prepare for the winter. The years examined in this modeling effort show two different summertime zooplankton scenarios. Periodic strong wind mixing events in the spring of 1995 prolonged the phytoplankton bloom resulting in tight pelagic coupling and a high biomass of calanoid copepods. A high copepod biomass developed in 1994 as well. Calm winds in 1996 led to a short, uncoupled phytoplankton bloom and low copepod biomass. The phytoplankton bloom in 1993 was also short and uncoupled. These springtime differences are manifested in the duration of the larval period for Pacific herring. Years with prolonged phytoplankton blooms and high calanoid biomass may lead to earlier larval metamorphosis, allowing more time for the herring to prepare for the overwintering fast.

Figure Legends:

Figure 1. Prince William Sound model domain, with an example of regions influenced by similar winds when the winds are blowing north at Potato Point. In this example, black is land, and the letters correspond to the following locations with measured winds: VZ, Valdez weather station; PP, Potato Point; BI, Bligh Island; MB, Mid-Sound buoy; CB, CLAB buoy; WH, Whittier; AR, Applegate Rocks; and MI, Middleton Island.

Figure 2. Wind pattern produced from using the Java tool, using the pattern shown in Figure 1, for a scenario with strong north winds observed at Potato Point.

Figure 3. Phytoplankton response to spatially varying wind fields in 1995.

Figure 4. Zooplankton response to spatially varying wind fields in 1995.

Figure 5. Phytoplankton response to spatially varying wind fields in 1996.

Figure 6. Zooplankton response to spatially varying wind fields in 1996.

Figure A-1. *Pseudocalanus* total biomass (mg wet weight/m^3) comparisons between two model formulations and field data.

Figure A-2. *Pseudocalanus* model total naupliar biomass (mg wet weight/m^3).

Figure A-3. Model stage-specific *Pseudocalanus* biomass (mg wet weight/m^3).

Figure B-1. Forcing data for the herring depth-integrated model. Top: Total small calanoid biomass in 1993 through 1996. Bottom: Mixed layer temperature. For clarity, only the extreme years are shown (1993 warm, 1995 cool).

Figure B-2. Length (mm) of larval Pacific herring from depth-averaged model for 1993-1996. Dashed lines show 60 days and metamorphosis length (25mm).

Figure B-3. Depth-resolving model results showing larval length after 60 days (solid) and 80 days (dashed) in the surface 50m. Note that lengths are greater in 1995 than in 1996, and that fish grow at deeper depths in 1995.

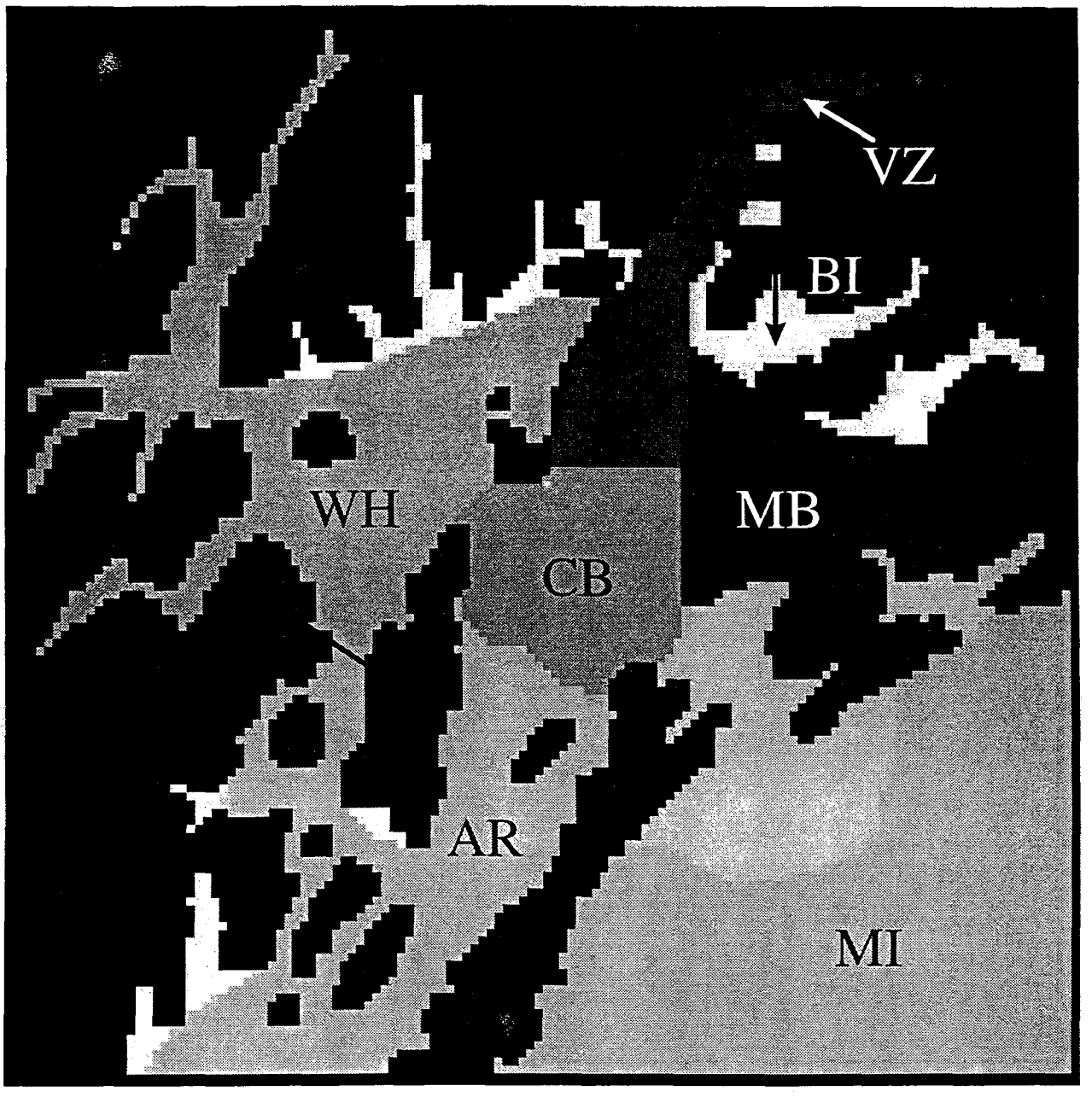

Figure 1: Prince William Sound model domain, with an example of regions influenced by similar winds when the winds are blowing north at Potato Point. In this example, black is land, and the letters correspond to the following locations with measured winds: VZ, Valdez weather station; PP, Potato Point; BI, Bligh Island; MB, Mid-Sound buoy; CB, CLAB buoy; WH, Whittier; AR, Applegate Rocks; and MI, Middleton Island.

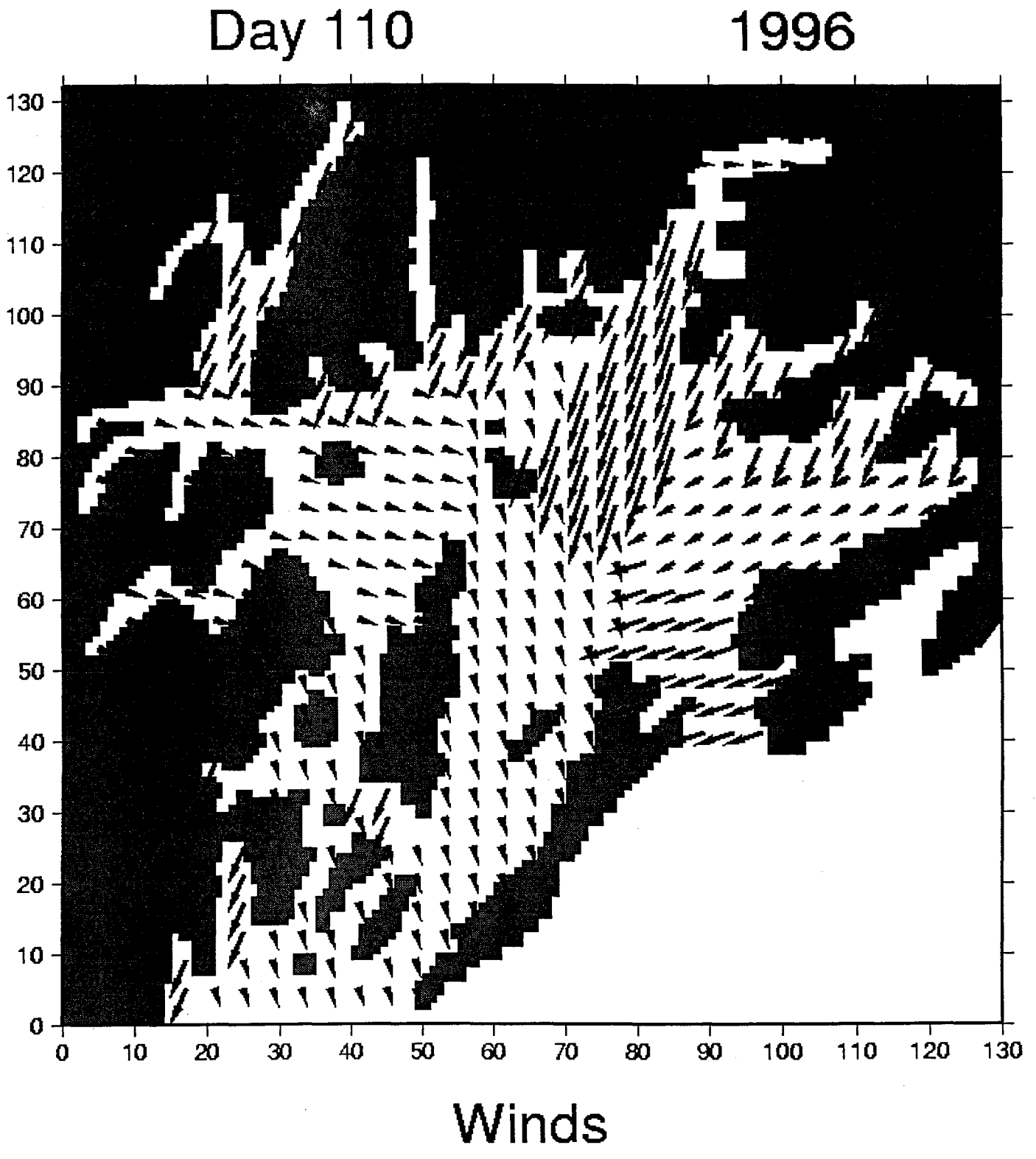
Day 110
1996
130
120
110
100
90
80
70
60
50
40
30
20
10
0
0
10
20
30
40
50
60
70
80
90
100
110
120
130
Winds

Figure 2:

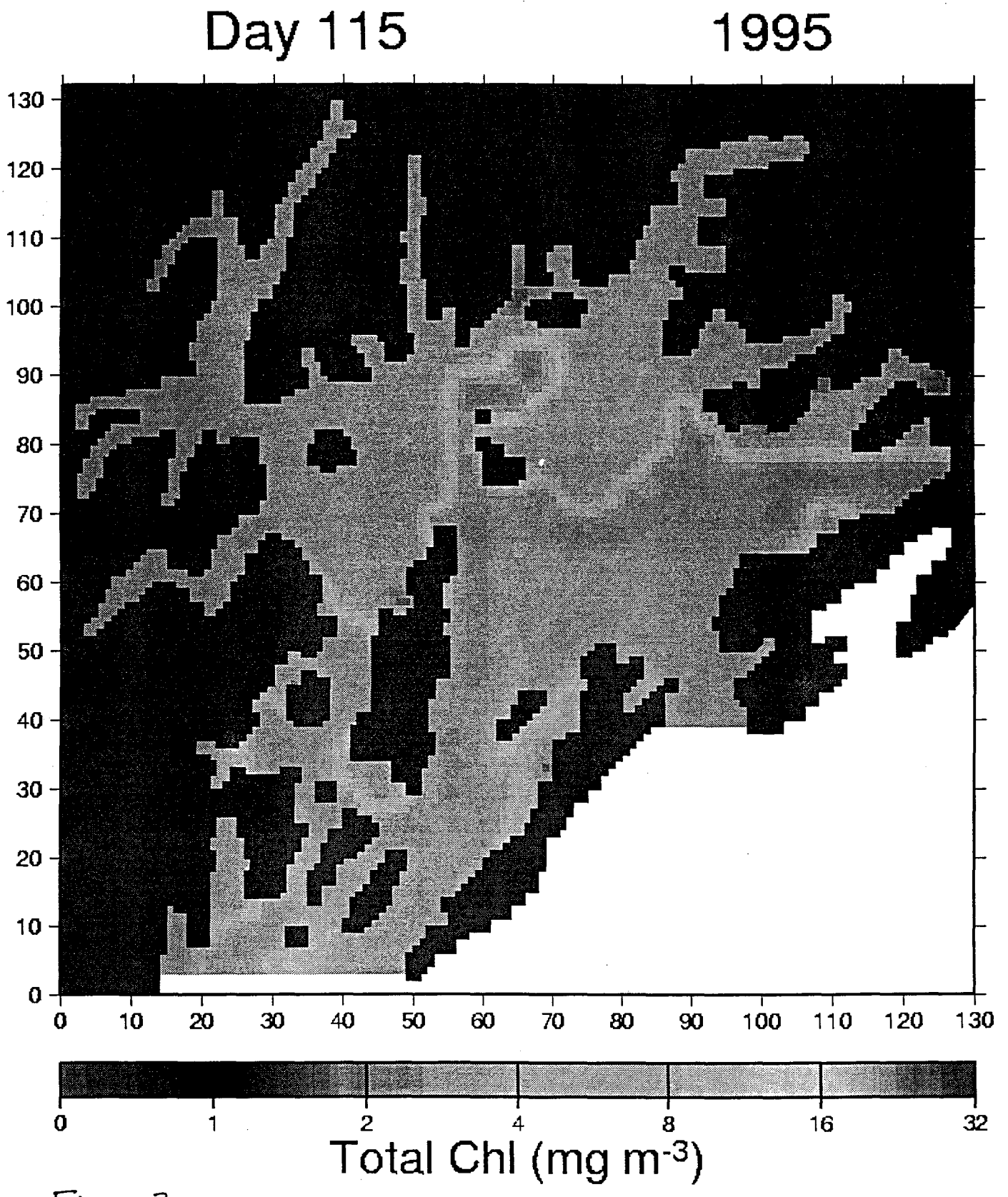
Day 115
1995
130
120
110
100
90
80
70
60
50
40
30
20
10
0
0
10
20
30
40
50
60
70
80
90
100
110
120
130
0
1
2
4
8
16
32
Total Chl (mg m-3)

Figure 3:

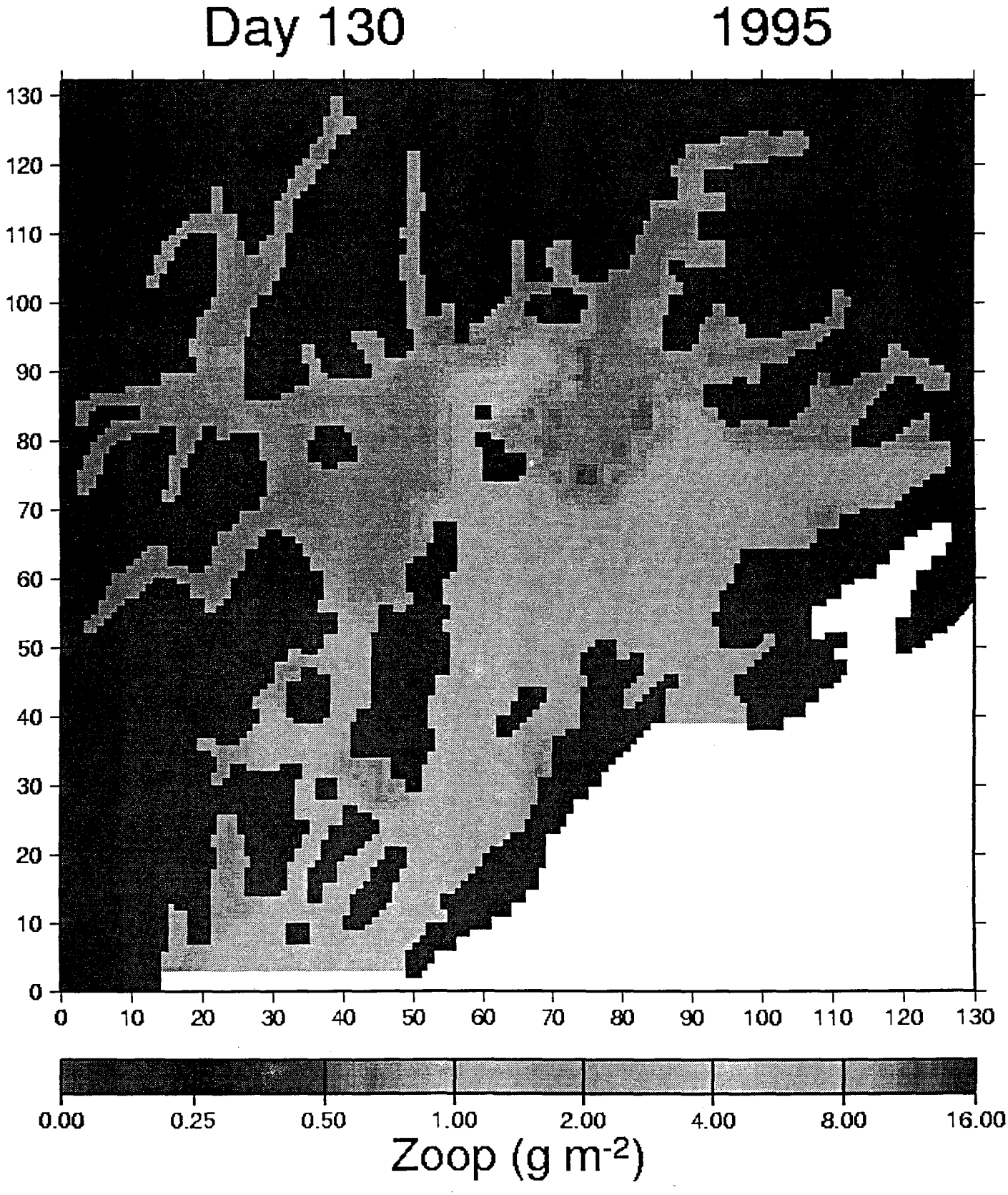
Day 130
1995
130
120
110
100
90
80
70
60
50
40
30
20
10
0
0
10
20
30
40
50
60
70
80
90
100
110
120
130
0.00
0.25
0.50
1.00
2.00
4.00
8.00
16.00
Zoop (g m-2)

Figure 4

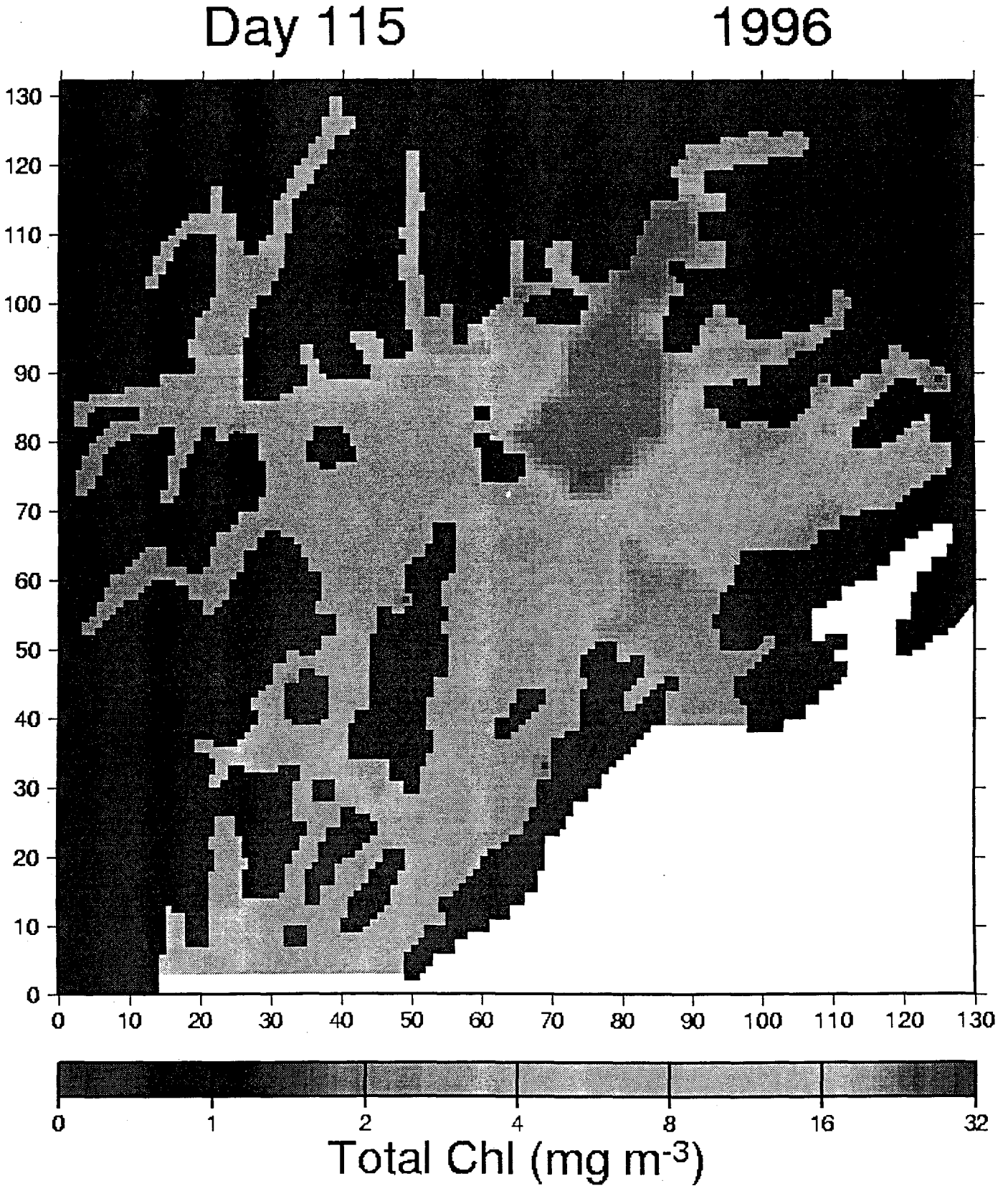
Day 115
1996
130
120
110
100
90
80
70
60
50
40
30
20
10
0
0
10
20
30
40
50
60
70
80
90
100
110
120
130
0
1
2
4
8
16
32
Total Chl (mg m-3)

Figure 5

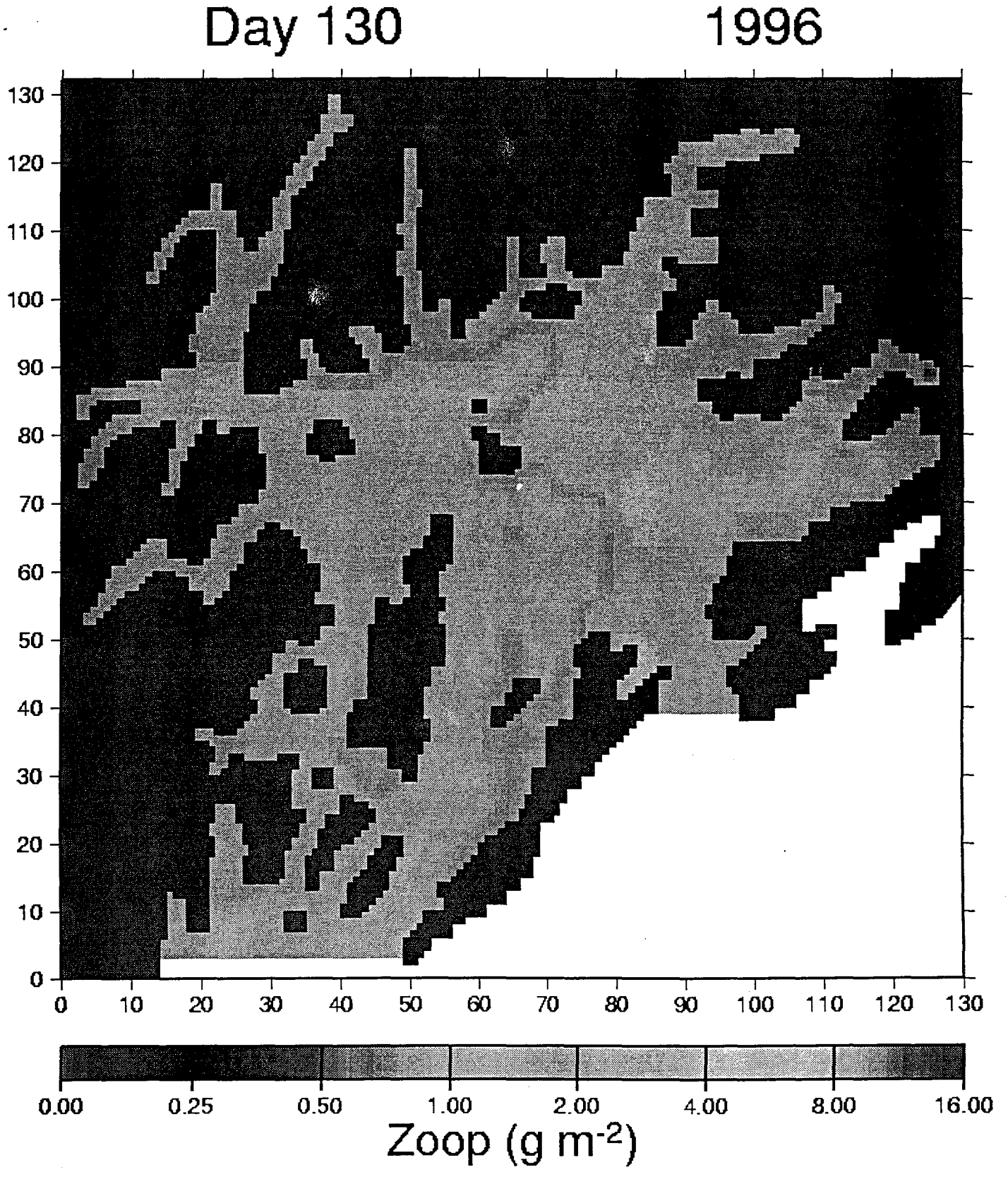
Day 130
1996
130
120
110
100
90
80
70
60
50
40
30
20
10
0
0
10
20
30
40
50
60
70
80
90
100
110
120
130
0.00
0.25
0.50
1.00
2.00
4.00
8.00
16.00
Zoop (g m-2)

Figure 6

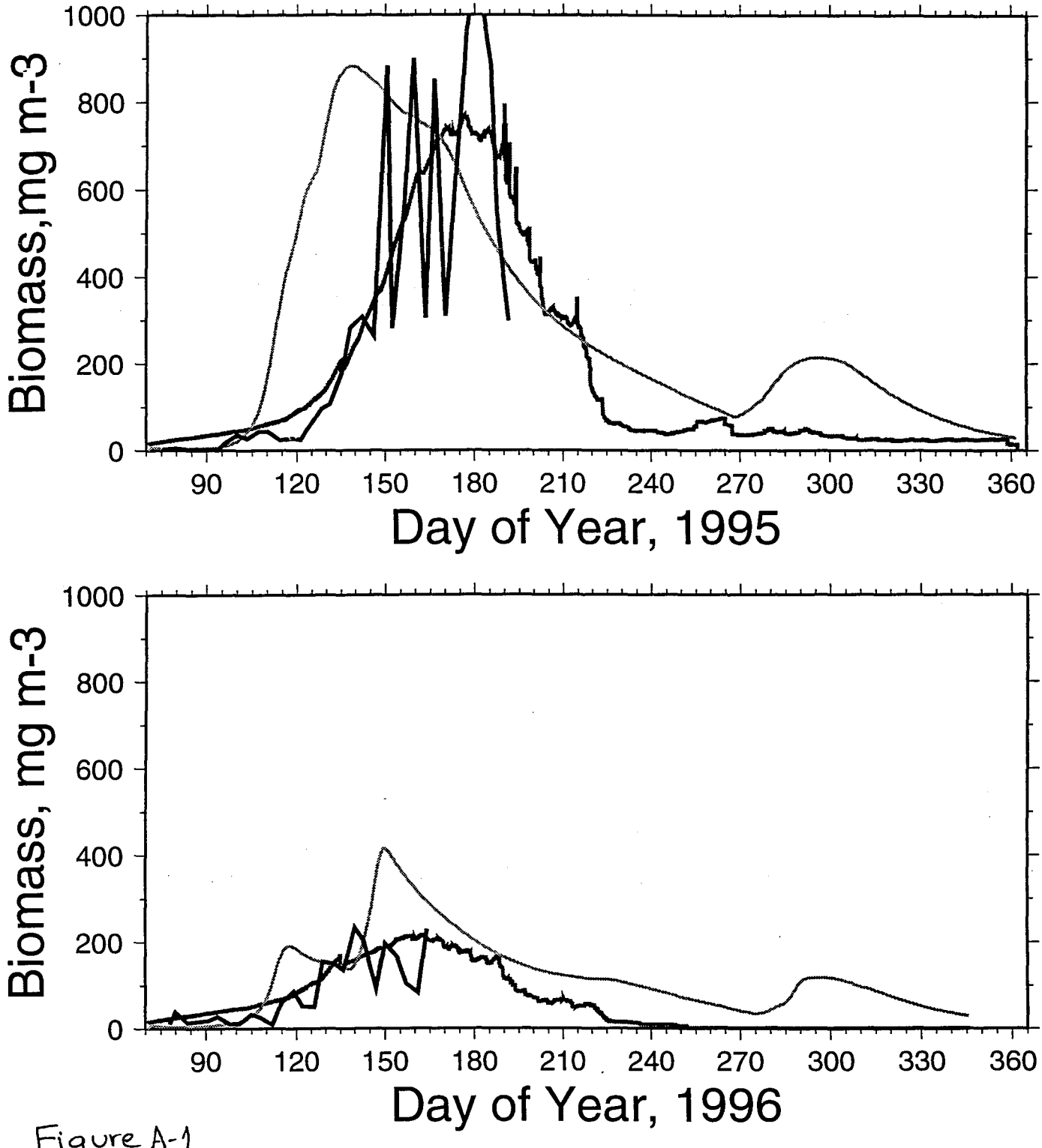

Figure A-1

— Field

— Model, 1st formulation: no life stages

— Model, 2nd formulation: with life stages

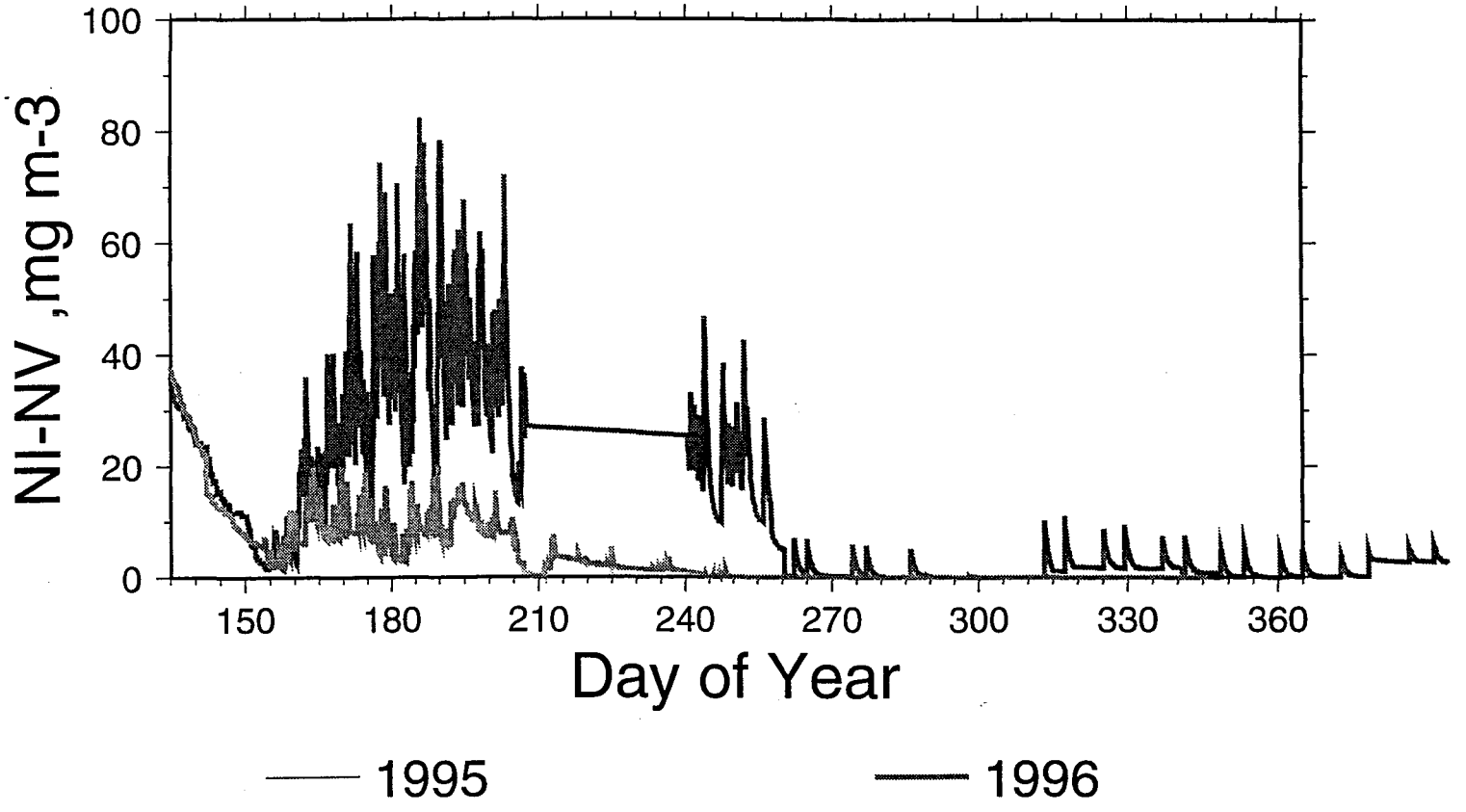
100
80
60
40
20
0
NI-NV ,mg m-3
150
180
210
240
270
300
330
360
Day of Year
1995
1996

Figure A-2.

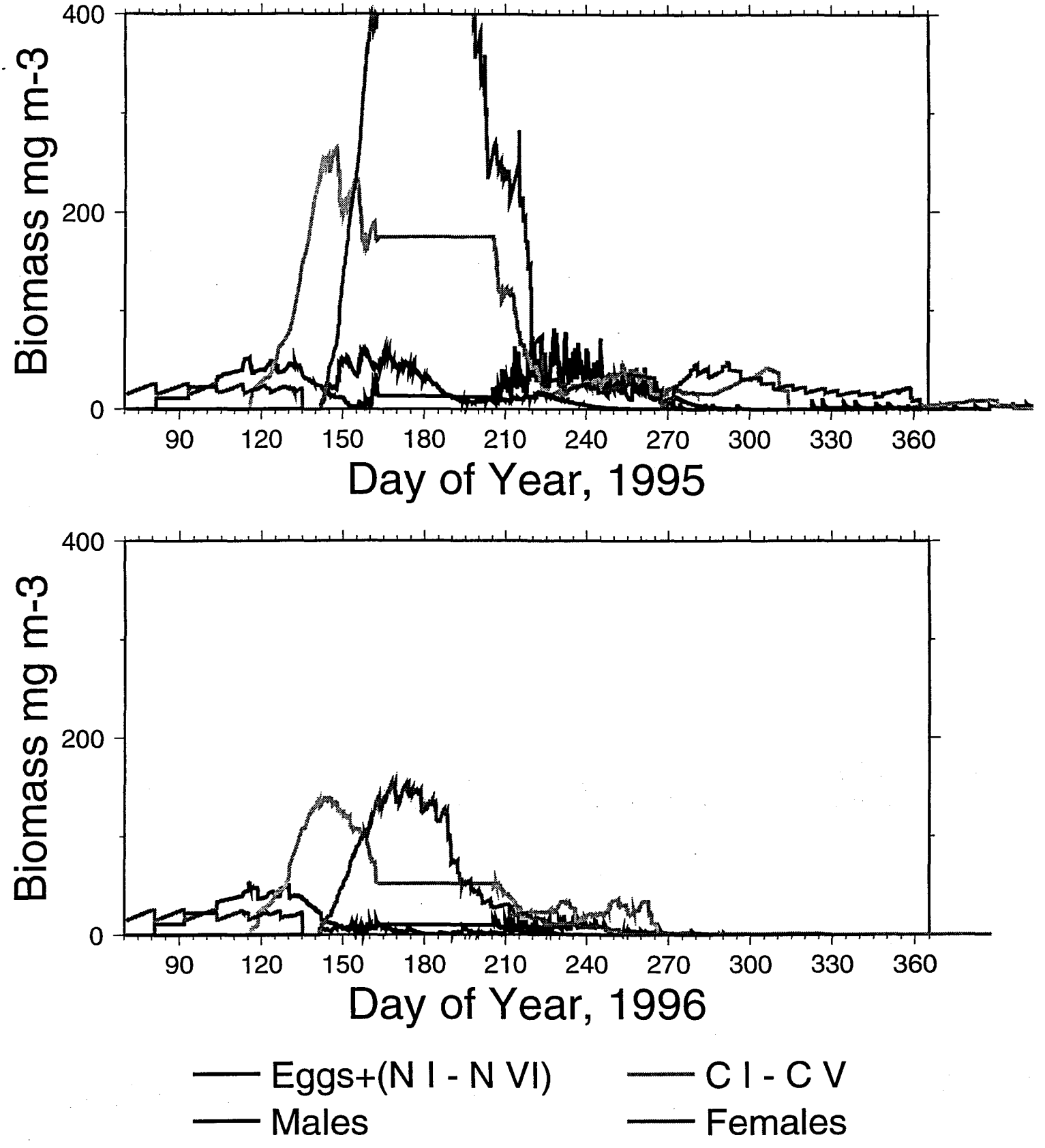
Biomass mg m-3
400
200
0
90
120
150
180
210
240
270
300
330
360
Day of Year, 1995
Biomass mg m-3
400
200
0
90
120
150
180
210
240
270
300
330
360
Day of Year, 1996
Eggs+(N I - N VI)
C I - C V
Males
Females

Figure A-3

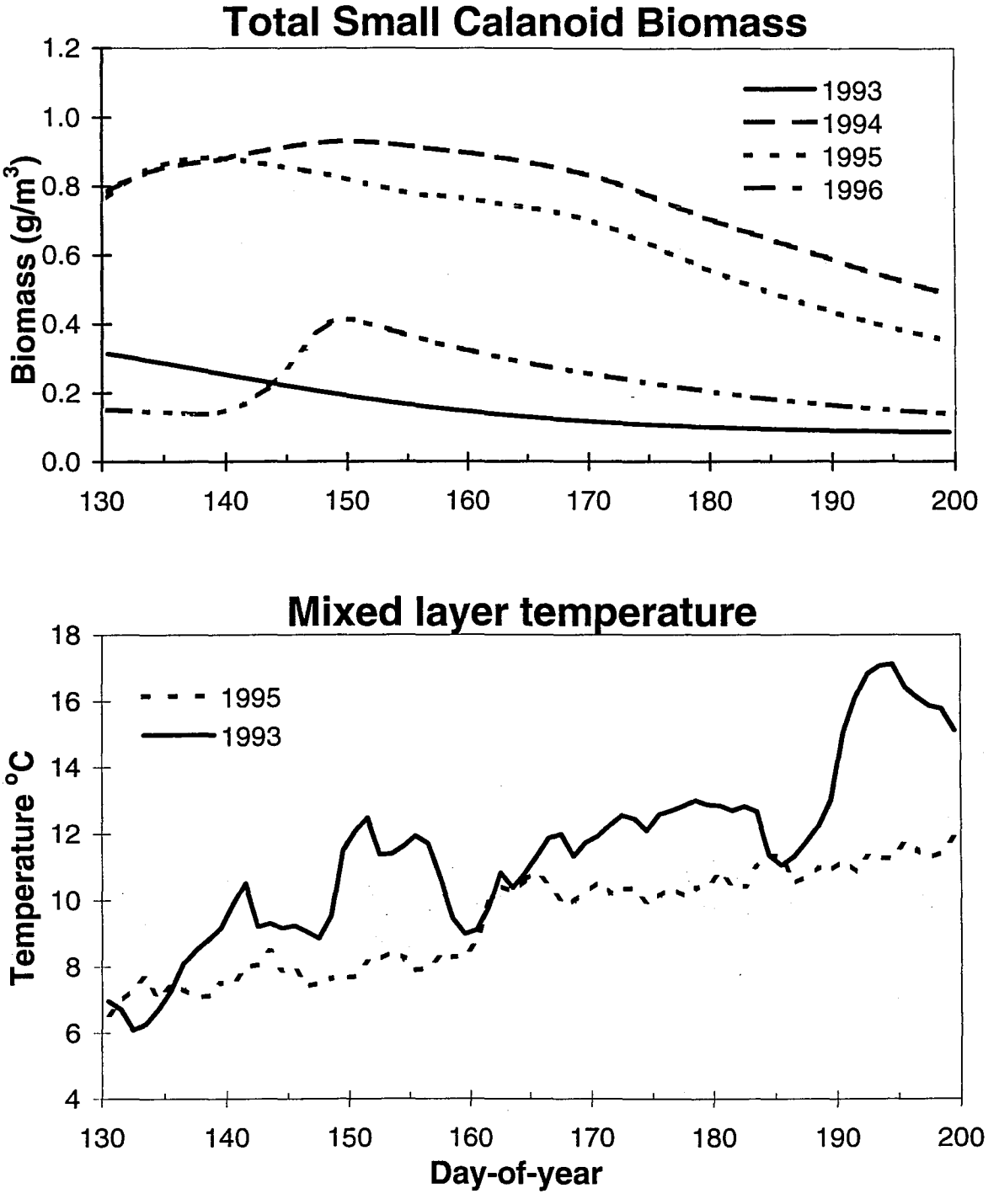

Figure B-1: Forcing data for the herring depth-integrated model. Top panel: Total small calanoid biomass in 1993 through 1996. Bottom panel: Mixed layer temperature. For clarity, only the extreme years are shown (warm 1993, cool 1995).

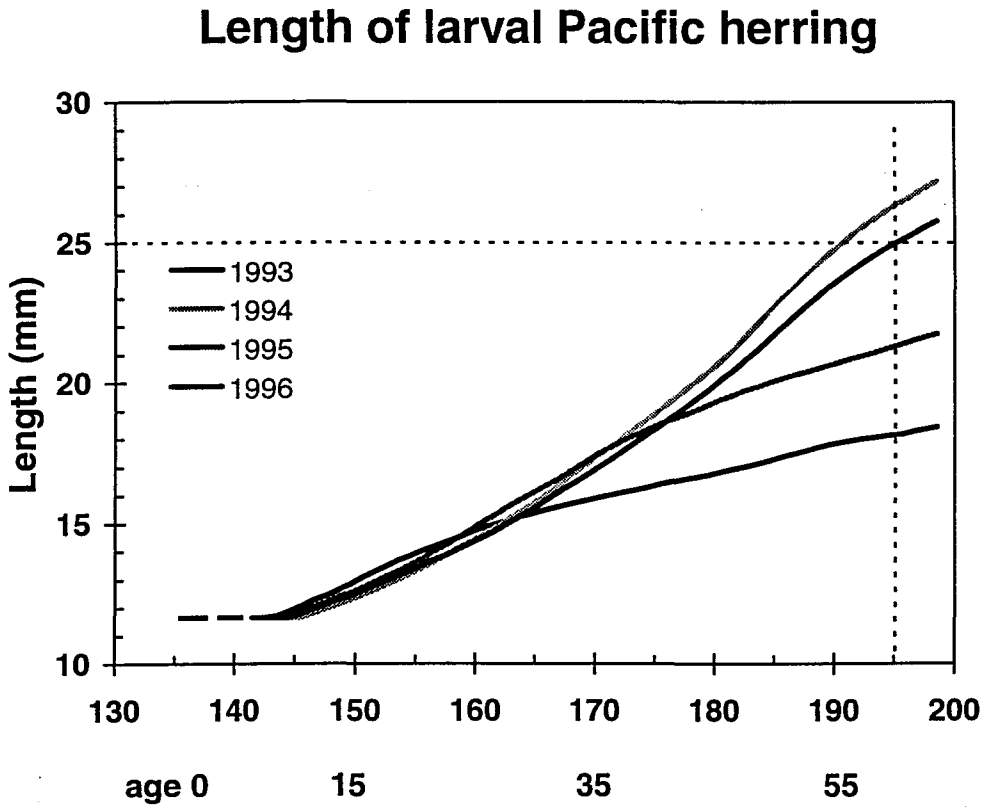

Figure B-2: Length (mm) of larval Pacfic herring from depth-averaged model for 1993-1996. Dashed lines show 60 days and metamorphosis length (25mm).

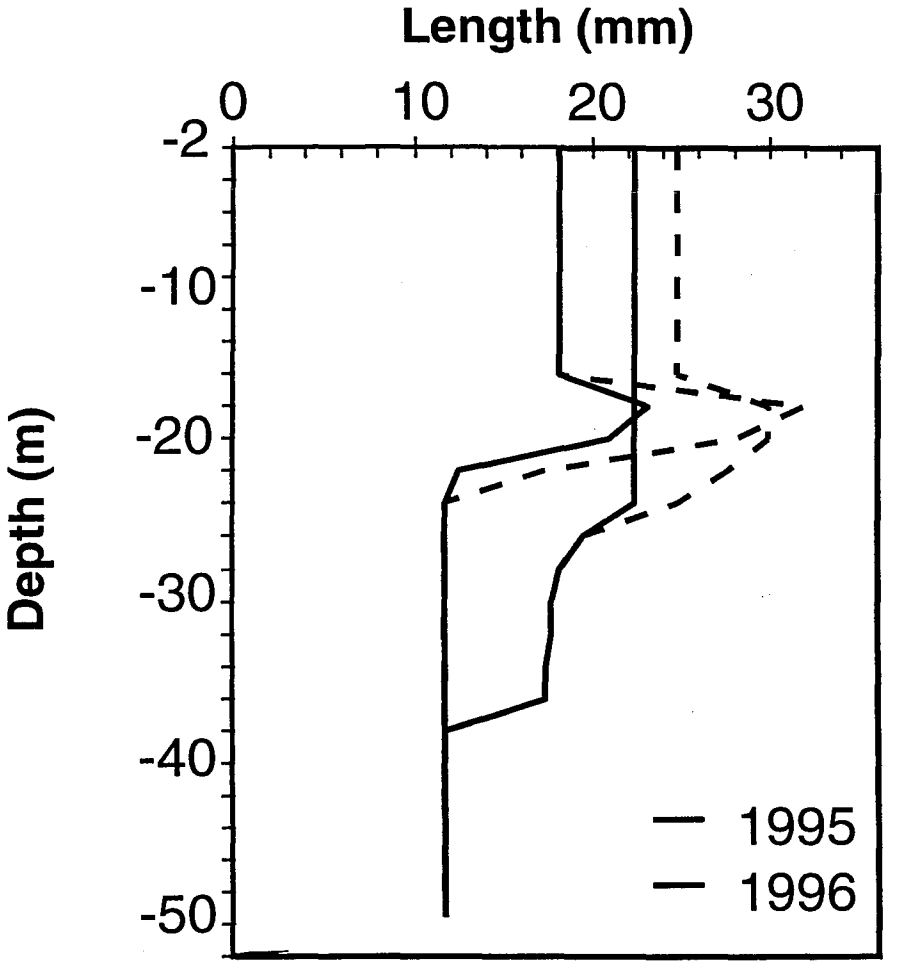

Figure B-3: Depth-resolving model results showing larval length after 60 days (solid) and 80 days (dashed) in the surface 50m. Note that lengths are greater in 1995 than 1996, and that fish grow at deeper depths in 1995.